Biochimica et Biophysica Acta, 1070 (1991) 419–428

BBAMEM 75459

A comparative study on interactions of α-aminoisobutyric acid containing antibiotic peptides, trichopolyn I and hypelcin A with phosphatidylcholine bilayers

Katsumi Matsuzaki [1], Takahide Shioyama [1], Emiko Okamura [2], Junzo Umemura [2], Tohru Takenaka [2], Yoshihisa Takaishi [3], Teturo Fujita [1] and Koichiro Miyajima [1]

[1] *Faculty of Pharmaceutical Sciences, Kyoto University, Sakyo-ku, Kyoto (Japan),* [2] *Institute for Chemical Research, Kyoto University, Uji, Kyoto (Japan) and* [3] *Faculty of Pharmaceutical Sciences, Tokushima University, Sho-machi, Tokushima (Japan)*

(Received 13 June 1991)

Key words: Trichopolyn I; Hypelcin A; Phosphatidylcholine bilayer; Permeability; Conformation; Orientation

Interactions of α-aminoisobutyric acid containing antibiotic peptides, trichopolyn I and hypelcin A with phosphatidylcholine bilayers were investigated to obtain some basic information on their bioactive mechanisms. Trichopolyn I as well as hypelcin A induced the leakage of a fluorescent dye, calcein, entrapped in sonicated egg yolk L-α-phosphatidylcholine vesicles. A quantitative analysis revealed that both the binding affinity and the 'membrane-perturbing activity' of trichopolyn I to the vesicles are about one-third of those of hypelcin A. The conformations and the orientations of the peptide and lipid molecules in the membranes were studied using polarized Fourier transform infrared-attenuated total reflection spectroscopy, circular dichroism, and differential scanning calorimetry. In phosphatidylcholine bilayers, both peptides mainly conformed to helical structures irrespective of the membrane physical state (gel or liquid-crystalline). The helix axes, penetrating the hydrophobic region of the bilayers, were oriented neither parallel nor perpendicular to the membrane normal. The disruption in the lipid packing induced by the peptide insertion seems to be responsible for the leakage by these peptides.

Introduction

Trichopolyn I is an α-aminoisobutyric acid (Aib) containing antibiotic peptide isolated from *Trichoderma polysporum* [1,2]. Its chemical structure (Fig. 1) is unique in that (1) all constituent amino acid residues have hydrophobic side chains, (2) two fatty acids are attached to the N-terminal portion, and (3) the C-terminal residue is trichodiaminol. The peptide inhibits the growth of Gram-positive bacteria and fungi [2] and uncouples oxidative phosphorylation in rat liver mitochondria (Terada, H. et al., unpublished work). These bioactivities may be explained on the basis of an increased permeability of bacterial or mitochondrial membranes. Other Aib containing peptides also show similar membrane-modifying properties, including ion channel formation and hemolysis [3–12]. The investigation of the interactions of trichopolyn I with lipid bilayers will give us some basic information on the molecular mechanisms for these activities.

Liposomes, a simple model for biomembranes, are a useful system for understanding peptide–lipid interactions. A change in membrane permeability, measured by the leakage of a fluorescent marker trapped within liposomes, can be correlated to conformational changes in both peptides and lipids, as detected by various spectroscopic and thermal techniques [11,13–17]. Especially, Fourier transform infrared (FTIR) spectroscopy is a powerful tool because conformations and intermolecular interactions can be detected nonperturbingly at a level of atomic groups [18,19]. Furthermore, the polarized attenuated total reflection (PATR) technique informs us of the orientation of each functional group independently [20–30].

Abbreviations: Aib, α-aminoisobutyric acid; FTIR, Fourier transform infrared; PATR, polarized attenuated total reflection; egg PC, egg yolk L-α-phosphatidylcholine; DPPC, L-α-dipalmitoylphosphatidylcholine; SUV, small unilamellar vesicle; CD, circular dichroism; DSC, differential scanning calorimetry.

Correspondence: K. Matsuzaki, Faculty of Pharmaceutical Sciences, Kyoto University, Sakyo-ku, Kyoto, 606-01, Japan.

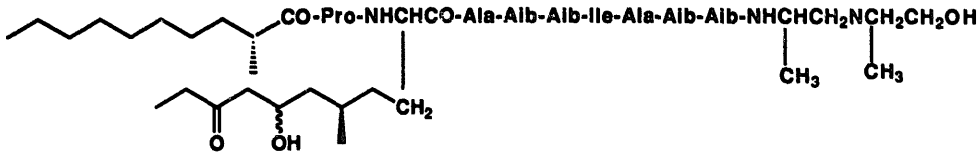

Fig. 1. Primary structure of trichopolyn I. Aib, α-amino-isobutyric acid.

In this study, an enhancement in the permeability of egg yolk L-α-phosphatidylcholine (egg PC) small unilamellar vesicle (SUV) membranes induced by trichopolyn I was examined in detail to obtain the affinity of the peptide to the membranes and the 'membrane-perturbing activity' of the peptide [11,16,17]. The results will be compared with data on hypelcin A, an Aib containing icosapeptide [11]. The conformations and the orientations of these peptides in phosphatidylcholine bilayers and the peptide induced disruption of the lipid packing were estimated using the FTIR-PATR method. Based on these results with data from circular dichroism (CD) and differential scanning calorimetry (DSC) studies, we will discuss trichopolyn I–lipid bilayer interactions compared with the case of hypelcin A [11].

Materials and Methods

Materials. Trichopolyn I and hypelcin A were isolated from *Trichoderma polysporum* [1,2] and *Hypocrea peltata* [3,4], respectively. Egg PC and L-α-dipalmitoylphosphatidylcholine (DPPC, > 99%) were purchased from Sigma. Calcein (3,3'-bis[*N*,*N*-bis(carboxymethyl)-aminomethyl]fluorescein) and spectrograde organic solvents were supplied by Dojindo (Kumamoto, Japan). Ammonium *d*-camphor-10-sulfonate and palmitic acid were products of Katayama (Osaka, Japan) and of Nippon Oils & Fats (Tokyo), respectively. Deuterium oxide (100%) was obtained from Aldrich. All other chemicals from Wako (Tokyo, Japan) were of special grade. A 10 mM Tris-HCl/150 mM NaCl/1 mM EDTA buffer (pH 7.0) was prepared with water twice-distilled from a quartz still.

Leakage from SUVs. Calcein entrapped SUVs were prepared by a sonication-gel filtration method as described elsewhere [11,16]. Briefly, a lipid film, after overnight vacuum drying, was hydrated with a 70 mM calcein solution (pH 7.0). The suspension was vortexed, followed by sonication in ice-water with nitrogen bubbling for 20 min using a titanium tip sonicator (Tomy UD-200). After centrifugal metal-debris removal, untrapped calcein was removed by gel filtration (Sephadex G-50, the buffer being used as an eluent). The separated vesicles were mixed with calcein-free sonicated vesicles to obtain the desired lipid concentration. The lipid concentration was determined by phosphorus analysis [31]. Small aliquots of a 2 mM trichopolyn I/methanol solution were added into 3 ml of the vesicular suspension while stirring in a thermostated (30 ± 0.5°C) quartz cuvette. The methanol concentration was less than 3% (v/v). The leakage of calcein from the vesicles was fluorometrically monitored (excitation at 490 nm and emission at 520 nm [32]). The fluorescence intensity corresponding to 100% leakage was determined by adding 150 μl of a 10% (v/v) Triton X-100 solution. Percent leakage was calculated after volume correction for dilution.

CD. Egg PC sonicated vesicles (1.5 mM) were prepared using the buffer as a hydrating medium. Small aliquots (2.5% (v/v)) of a 2 mM trichopolyn I/methanol solution were added to the vesicle suspension or the buffer. The CD spectra were recorded on a computerized Jasco J-600 instrument. The instrumental outputs were calibrated using non-hygroscopic ammonium *d*-camphor-10-sulfonate [33]. A quartz cuvette of 1-mm path length was thermostated at 30 ± 0.5°C. Eight scans were averaged for each sample. Averaged blank spectra (the vesicle suspension or the buffer) were subtracted to yield the 'pure' spectra of the peptide. The reported spectra were the average of three independent preparations for each type of sample. The standard deviations were indicated by error bars.

DSC. DPPC (3 mg) and trichopolyn I (0–0.5 mg) were weighed into an aluminum pan. A drop of chloroform/methanol (1:1, v/v) was added to dissolve the peptide and the lipid. The solvent was removed by overnight drying. After water addition (30 μl), the hermetically sealed sample was heated at 60°C for 10 min and then cooled to room temperature. The heating-cooling procedure was repeated twice. The DSC thermogram of the sample was recorded on a Shimadzu DT-30 thermal analyzer with a SC-30 unit at a heating rate of 10 C°/min. The heat and the temperature outputs were calibrated with palmitic acid.

FTIR-PATR spectroscopy. Cast dry films of DPPC or DPPC/peptide (20:1, mol/mol) were prepared by uniformly spreading a chloroform/methanol solution (0.4 ml) of 20 mM DPPC or 20 mM DPPC/1 mM peptide on one face of a germanium ATR plate ($52 \times 18 \times 2$ mm) followed by gradual evaporation of the solvent. The film thickness estimated from the applied amount of the lipid was about 6 μm. The plate was then placed in a thermostated homemade Teflon cell consisting of three parts (I–III), as shown in Fig. 2 [28].

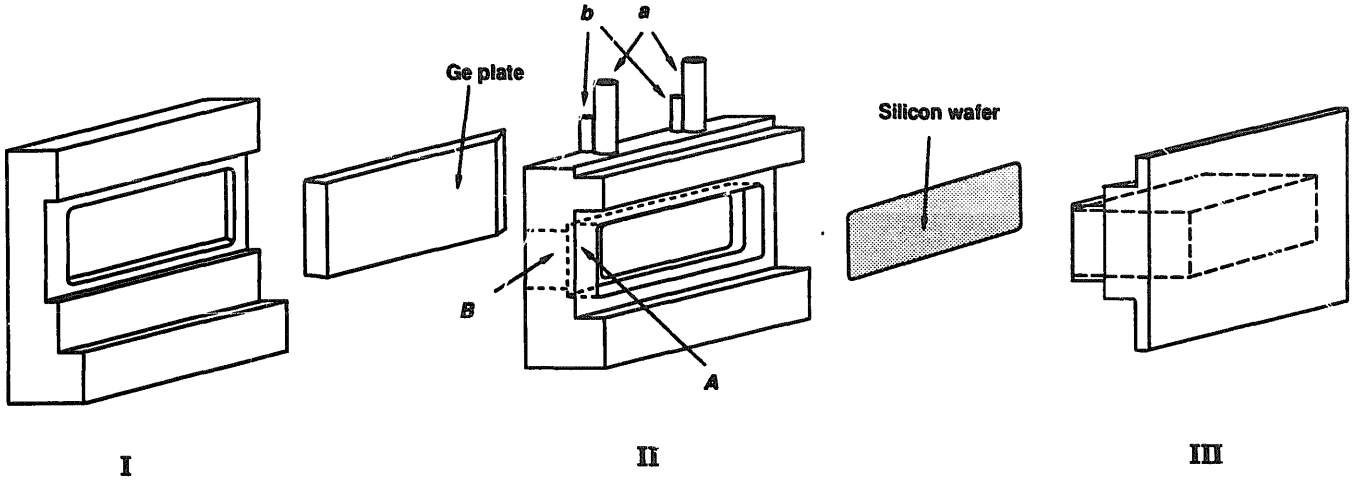

Fig. 2. Illustration of the Teflon cell for the FTIR-PATR experiment.

The germanium plate was sandwiched between Parts I and II so that the film coated side of the plate faced Part II. Part II has two compartments, *A* and *B*, separated by a silicon wafer. which is fixed by Part III. D_2O for hydration was injected into Compartment *B* through Pipes *b*. A thermostated ethylene glycol/water (1 : 1, v/v) was circulated into Compartment *A* through Pipes *a*. The temperature in Compartment *B* was directly monitored with an inserted copper-constantan thermocouple. The accuracy of the temperature control and reading was within ± 0.1 C°.

The temperature-dependent spectroscopic study was performed as follows: After the thermostated cell was mounted in the spectrophotometer chamber, the spectra of the dry film were recorded. The film was then hydrated with D_2O (2 ml) for 1 h at 50°C. We confirmed that this condition was sufficient for complete hydration. The sample was cooled to 20°C, and subjected to FTIR-PATR measurements in the temperature range 20–55°C. Spectra were recorded on a Nicolet 6000C FTIR spectrophotometer equipped with an Hg-Cd-Te detector. To minimize spectral contributions of atmospheric water vapor, the instrument was purged with dry air. PATR measurements were carried out using a Perkin-Elmer multiple ATR attachment and an AgBr polarizer. The angle of incidence was 45° and the number of total reflections was 12 on the film side. Three hundred interferograms collected with a maximum optical retardation of 0.25 cm were accumulated with a resolution of 4 cm^{-1}. Subtraction of gently sloping water vapor bands was accomplished to improve the background prior to the frequency measurement. The accuracy of the frequency reading was better than ± 0.1 cm^{-1}. The dichroic ratio, defined by $\Delta A_{\parallel}/\Delta A_{\perp}$ was calculated from the polarized spectra. The absorbance (ΔA) was obtained as the peak height of each absorption band. The subscripts $\parallel$ and $\perp$ refer to polarized light with its electric vector parallel and perpendicular to the plane of incidence, respectively. The base line method was used to minimize the back ground artifact. See Appendix for details.

Results

Leakage

Addition of trichopolyn I caused an efflux of calcein, a fluorescent marker trapped within egg PC SUVs. Membrane-lytic peptides alter lipid membrane permeability in two steps, i.e. the binding of the peptide to the membrane and the ensuing membrane disruption. Accordingly, two determinants of the leakage are (1) the membrane affinity of the peptide (the binding isotherm) and (2) its membrane-perturbing activity. These factors can be obtained by analyzing both the peptide concentration and the lipid concentration dependences of the leakage rate [11,16,17]. Fig. 3 shows these dependences. An increase in the peptide concentration or a decrease in the lipid concentration resulted in an enhanced leakage rate, suggesting that the amount of the membrane-bound peptide per lipid molecule, *r*,

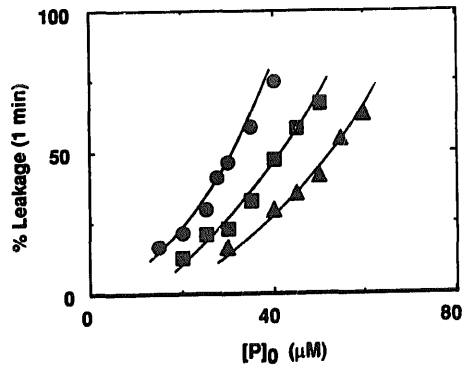

Fig. 3. Dependence of calcein leakage rate on peptide and lipid concentrations for trichopolyn I-egg PC SUV system at 30°C. The calcein leakage rate, defined as the percent leakage for the initial (first) minute, is plotted as a function of the peptide concentration, $[P]_0$, at different lipid concentrations, [L]. [L] (μM): ●, 518; ■, 885; ▲, 1230.

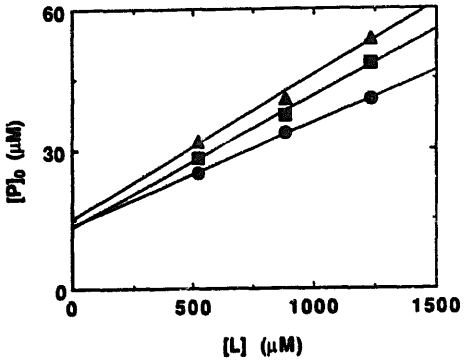

Fig. 4. Estimation of free and membrane-bound peptide concentrations. Three pairs of $[P]_0$ and [L] values where a given leakage rate was observed were obtained from Fig. 3. $[P]_0$ is plotted against [L] according to the equation in the text. The free peptide concentration, $[P]_f$, and the amount of membrane-bound peptide per lipid molecule, r, were evaluated from the intercept and the slope, respectively. Leakage rate (the percent leakage for the initial (first) minute: ●, 30; ■, 40; ▲, 50. The lines are least-squares fits.

determines the leakage rate. Here the leakage rate defined as the percent leakage for the initial 1 min is used as a measure of the initial leakage rate because the true rate was too rapid to precisely measure without a stopped-flow apparatus. The amount, r, can be connected to experimental conditions (the total peptide concentration, $[P]_0$, and the lipid concentration, [L]) through a material balance equation:

$$[P]_0 = [P]_f + r[L]$$

where $[P]_f$ is the free peptide concentration. A pair of r and $[P]_f$ values corresponding to a given leakage rate can thus be estimated with three sets of $[P]_0$ and [L] values where the leakage rate was observed. Fig. 4 shows that the $[P]_0$ vs. [L] plots at any given leakage rates gave linear relations (the square correlation coefficients were greater than 0.99). The r and $[P]_f$ values were obtained from the slopes and the intercepts, respectively. Fig. 5a shows the r-$[P]_f$ relationship thus estimated (i.e., the binding isotherm) with data for the hypelcin A-egg PC SUV system [11]. The slope ($2.0 \cdot 10^3$ M^{-1}) of the linear isotherm was about one-third of that of hypelcin A ($6.6 \cdot 10^3$ M^{-1}), indicating a smaller affinity of trichopolyn I. The scatter of the data for trichopolyn I is ascribable to the indirect estimation of the binding isotherm. The errors in $[P]_f$ and r were estimated to be ±20% and ±10%, respectively. Fig. 5b illustrates the leakage rate-r relationship, i.e. the membrane-perturbing activity of the peptide [11,16,17]. The leakage requires the binding of one trichopolyn I molecule to 30–50 lipid molecules. The membrane-perturbing activity of the peptide was also approx. one-third of that of hypelcin A. During the leakage, neither a change in 90° light scattering intensity nor lipid mixing [12] was observed, demonstrating that neither the complete solubilization nor the fusion of the vesicles occurred (data not shown).

Our preliminary study found that trichopolyn I as well as hypelcin A caused hemolysis of porcine erythrocytes. The peptide concentrations necessary for 50% hemolysis were 25 and 15 μM for trichopolyn I and hypelcin A, respectively (1% (v/v) erythrocytes in a phosphate-buffered saline, 1 h incubation at 37°C). The hemolytic activity of trichopolyn I was again weaker than that of hypelcin A.

CD

The conformational change of trichopolyn I upon binding to egg PC membranes was estimated on the basis of its CD spectra (Fig. 6). In the buffer, the spectrum suggested that the peptide is in an unordered conformation. A CD spectrum measured at 5 μM was superimposable onto the spectrum in Fig. 6, indicating that the peptide is soluble in the buffer up to 50 μM with its conformation unaltered. Addition of egg PC SUVs appeared to drastically change the CD spectrum. Under this condition, about three-fourths of the pep-

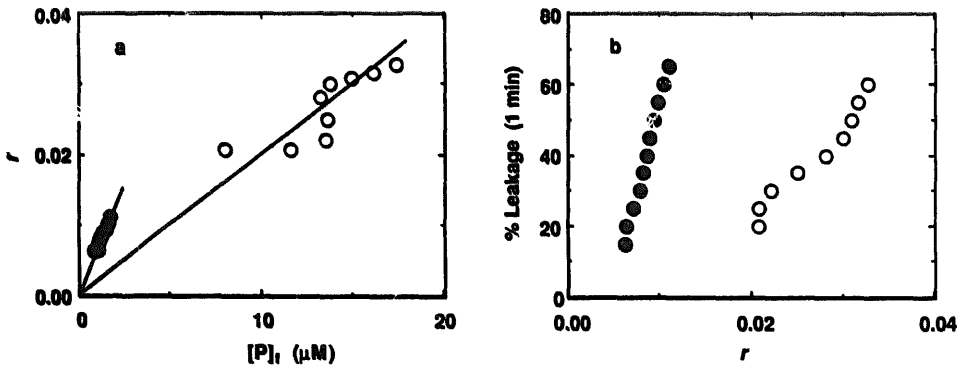

Fig. 5. Quantitative analysis of trichopolyn I and hypelcin A induced leakage at 30°C. The relationships (a) between the amount of the membrane-bound peptide per lipid molecule, r, and the free peptide concentration, $[P]_f$, (i.e. binding isotherms) and (b) between the leakage rate and r are shown. The leakage rate is expressed as the percent leakage for the initial 1 min. Peptides: ○, trichopolyn I; ●, hypelcin A. Data for hypelcin A were taken from Ref. 11.

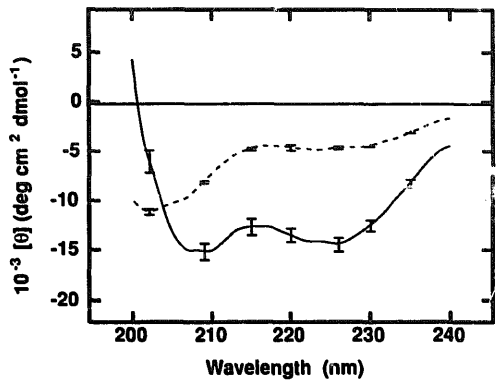

Fig. 6. CD spectra of trichopolyn I in the absence and presence of egg PC SUVs at 30°C. The CD spectra of a 50 μM trichopolyn I/buffer solution were recorded in the absence (dashed line) and presence (solid line) of 1.5 mM egg PC SUVs. The error bars indicate standard errors for three independent preparations.

tide molecules present are membrane-bound (Fig. 5a). Prior to the interpretation of this spectral change, however, the contribution of optical artifacts should be clarified: in vesicle suspensions, CD spectra may be distorted by two optical effects, differential light scattering and differential absorption flattening [34,35]. These artifacts are found to be negligible in our experimental condition, as discussed elsewhere [11]. The observed spectral change included the conspicuousness of double minima around 209 and 225 nm, suggesting an increase in the helical content. A similar change has been reported for other Aib containing peptides, alamethicin [36–38] and hypelcin A [11]. Unfortunately, for these peptides, the helical content cannot be reasonably estimated using a conventional least-squares curve fitting procedure [39], as reported previously [11,36,38].

DSC

The effects of trichopolyn I on the gel to liquid-crystalline phase transition of DPPC bilayers were examined using the DSC technique. The phase transition

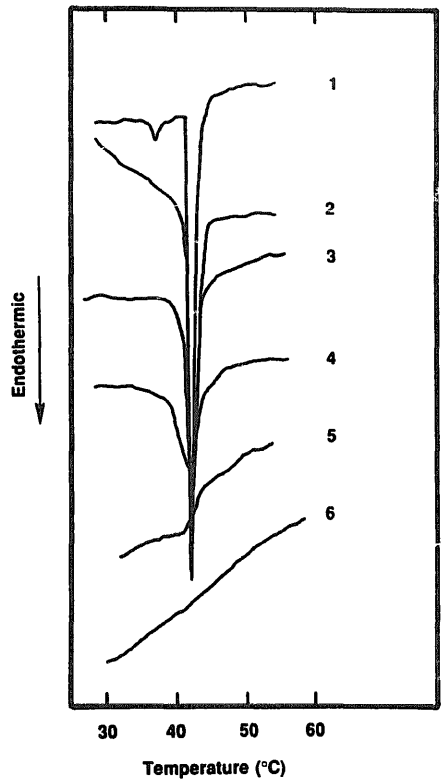

Fig. 7. DSC heating curves of trichopolyn I incorporated DPPC vesicles. The heating rate was 10 C° min^{-1}. Peptide content (mol%): curve 1, 0; curve 2, 1.4; curve 3, 2.9; curve 4, 4.9; curve 5, 7.2; curve 6, 9.3.

reflects the modification of the lipid-lipid interactions. Fig. 7 depicts the DSC heating curves of the DPPC membranes for different peptide contents. In the absence of the peptide (curve 1), a sharp onset of the main transition appeared at 41°C with a pretransition at 35°C, typical of DPPC multilamellar vesicles [40]. Similar to the hypelcin A-DPPC system [11], incorporation of trichopolyn I resulted in the disappearance of the pretransition and a broadened DSC curve with a reduced transition enthalpy (curves 2–5). At a peptide content of 9.3 mol%, the phase transition was com-

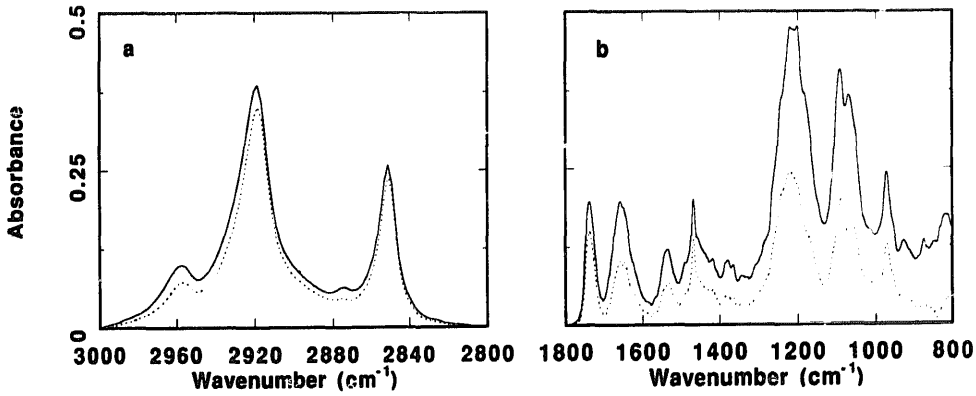

Fig. 8. FTIR-PATR spectra of a DPPC/hypelcin A (20:1, mol/mol) film fully hydrated with D_2O, for the IR beam with its electric vector parallel (solid line) and perpendicular (broken line) to the plane of incidence at 22.5°C. (a) The methylene stretching region and (b) the amide I′ and polar headgroup region.

pletely abolished (curve 6). These phenomena have been often observed for peptides or proteins interacting with the hydrophobic region of the membranes [41–44].

FTIR-PATR spectroscopy

We examined the peptide–lipid interactions at a molecular level using the FTIR-PATR technique. This method can elucidate orientations as well as conformations of both peptide and lipid molecules [20–25,27–30]. Fig. 8 shows an example of polarized spectra of a DPPC/hypelcin A (20:1, mol/mol) film *fully hydrated* with D_2O, measured at 22.5°C.

First, the methylene stretching bands will be considered. The frequencies of the methylene antisymmetric (≈ 2920 cm^{-1}) and symmetric (≈ 2850 cm^{-1}) stretching bands are known to be sensitive to *trans-gauche* conformations of the lipid acyl chains [19]. In peptide containing samples, absorptions due to peptide side chains often interfere with these bands. We estimated, by measuring the spectra of peptide cast films, that for both peptides, the contributions of the side chain bands to the methylene stretching region are less than 10% and about 15% near 2850 cm^{-1} and 2920 cm^{-1}, respectively. The methylene symmetric stretching vibration, less affected by the peptide bands, was used to investigate the conformation of the lipid hydrocarbon chain. The advantage of monitoring the symmetric stretching band has been described previously [19]. Fig. 9a depicts the temperature dependence of the frequency of the symmetric stretching band. After an experimental run, the sample was cooled again to 25°C, and then reheated to 50°C. We confirmed that the spectra were reproducible during this recooling-reheating cycle. For a pure DPPC film, the peak maximum exhibited an abrupt shift (≈ 1.5 cm^{-1}) to a higher frequency around 42°C, indicating the gel to liquid-crystalline phase transition increases the number of gauche conformers in the acyl chain [19]. A similar frequency shift has been reported for DPPC multilamellar vesicles suspended in a D_2O-containing buffer [45]. The error bars indicate the standard deviations estimated from three independent experiments. Addition of 5 mol% hypelcin A somewhat broadened the phase transition, but little affected the conformation. In contrast, incorporation of trichopolyn I solidified the acyl chains in the fluid state.

The orientation of the hydrocarbon chain was evaluated from the observed dichroic ratio using Eqn. A-6. For the methylene symmetric stretching band, the S' value is -0.5 [25]. Fig. 9b shows the temperature dependence of the S value (the order parameter of the hydrocarbon chain axis with respect to the plate normal). The order parameter for the DPPC membrane dropped at the phase transition temperature, coinciding with the frequency shift. The presence of the peptides reduced the order parameter in the whole temperature region. The effect of hypelcin A was more significant than that of trichopolyn I.

Second, the effects of the peptides on the lipid polar groups will be evaluated. The peptides had no interfering absorptions below 1100 cm^{-1}. The band assignable to the asymmetric stretching vibration of N-$(CH_3)_3$ was observed at ≈ 970 cm^{-1}. Neither the frequency nor the dichroic ratio was affected by the two peptides, suggesting these peptides do not interact strongly with the choline head group of DPPC. The symmetric PO_2^- stretching band appeared around 1090 cm^{-1}. For the pure DPPC bilayers, the peak position was changed slightly (1092 cm^{-1} in the gel phase to 1090 cm^{-1} in the liquid-crystalline state) when the membrane passes through the phase transition. This shift may be ascribable to an increased hydration in the fluid state [46]. The presence of 5 mol% hypelcin A red shifted the peak position by about 2 cm^{-1}, whereas addition of trichopolyn I blue shifted the maximum by 2–3 cm^{-1} over the whole temperature region. These results indicate that both peptides more or less influence the phosphate group of the lipid. The orientation of the polar group was not examined because of a significant

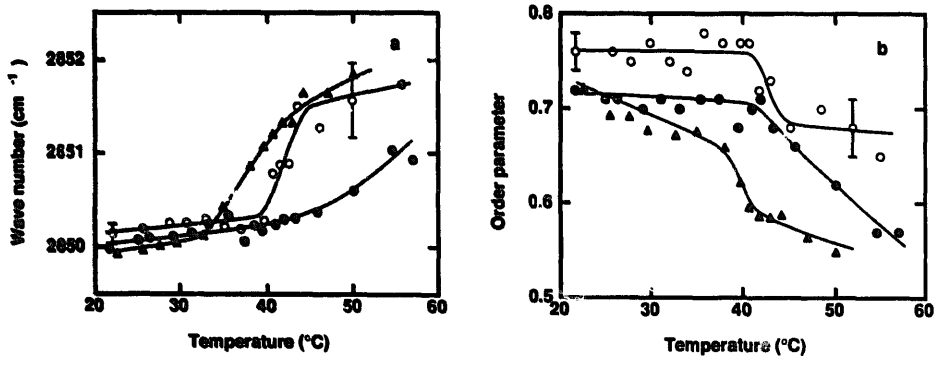

Fig. 9. Temperature dependences of parameters characterizing conformation and orientation of lipid hydrocarbon chain obtained from FTIR-PATR measurements. (a) The frequency of the methylene symmetric stretching band and (b) the order parameter of the hydrocarbon chain calculated from Eqn. (A-6). Symbols: ○, pure DPPC; ●, DPPC/trichopolyn I (20:1, mol/mol); ▲, DPPC/hypelcin A (20:1, mol/mol).

overlap of the adjacent R-O-P-O-R′ vibration around 1065 cm^{-1} [46].

Finally, the amide I′ bands of the peptides will be reported. The amide I′ band contour is sensitive to the secondary structure of a peptide [47]. The frequencies of the amide I′ bands of hypelcin A and trichopolyn I in DPPC membranes were 1659 and 1666 cm^{-1}, respectively, irrespective of the temperature. These frequencies are assignable to the α-helix and 3_{10}-helix, respectively [48]. Some 3_{10}-helix structure may be present in hypelcin A as in the case of alamethicin [49]. Our CD data (Ref. 11 and Fig. 6) support the conclusion that these peptides mainly adopt helical conformations in lipid bilayers. The dichroic ratios of the amide I′ bands were around 2.0 (1.9–2.2) over the whole temperature region. For the α-helix, the θ value has been estimated to be 27° [50]. The observed R values correspond to the S values of −0.043 to 0.079 (α, 56°–52°), suggesting that the helices distribute almost randomly or happen to be oriented at angles around the magic angle (54.7°) As for the θ value of the 3_{10}-helix, polarized IR spectra of an oriented 3_{10}-helical peptide [51] shows a parallel dichroism for the amide I′ band, suggesting a θ value smaller than the magic angle (judging from the spectra, the θ value may be around 45°) Thus, the above picture on the orientation of the helix also holds for the 3_{10}-helix. In the case of hypelcin A, if the whole molecule folds into a helix, the presence of Pro^{14} will bend the helix by an angle of approx. 20° [49]. The S value should be then divided by 0.95 $(=(14/20)+(6/20)(3\cos^2 20° - 1)/2)$. This correction never changes the above conclusion.

Discussion

Both trichopolyn I and hypelcin A are Aib containing hydrophobic peptides which exhibit similar bioactivities involving membrane-modifying properties [1–5,11,12]. However, they differ in molecular size and constituent amino acids. The molecular weight of trichopolyn I is about half of that of hypelcin A. Hypelcin A contains three polar amino acid residues (Gln) whereas trichopolyn I has no polar residues. Comparison between the interactions of the two peptides with lipid bilayers seems to be important for understanding the molecular machinery of the bioactivities.

Peptide conformation and orientation

The FTIR-PATR technique is a powerful tool for investigating peptide–lipid interactions because orientations as well as conformations of functional groups can be nonperturbingly estimated [20–25,27–30]. In this study, we measured the spectra of peptide–lipid films fully hydrated in the presence of excess D_2O. Under this condition, we should take into account the presence of the free peptide molecules. We estimated the fractions of the membrane-bound peptides based on the integrated intensity ratios of the carbonyl C = O stretching band of the lipid around 1740 cm^{-1} to the amide I bands, calculated using Eqn. A-2. Hydration reduced the ratios to 60–70% and 70–80% of those before hydration for trichopolyn I and hypelcin A, respectively. These reductions are ascribable to escape of the peptides from the membrane phase to the excess aqueous phase. The stronger binding of hypelcin A is consistent with the binding isotherm (Fig. 5a). Thus, the observed amide I′ bands are superpositions of the two spectra from the membrane-bound and the free peptides. The frequencies of the amide I′ bands of hypelcin A (1659 cm^{-1}) and trichopolyn I (1665 cm^{-1}) are characteristic of the α-helix and the 3_{10}-helix [48], in keeping with the CD data (Ref. 11 and Fig. 6). For Aib containing peptides, the 3_{10}-helix is preferred for shorter peptides (8 residues or less), whereas the α helix is preferred for longer peptides (9–20 residues) [52]. Membrane-associating peptides tend to fold in helical conformations in the lipid environments [11,13,15–17,38,53–56]. We estimated the orientations of the helices in the membranes based on the R values calculated from the peak height ratios of the amide I′ bands around 1660 cm^{-1}. The contributions to the R values from the free peptides seem to be much smaller than those expected from the free peptide fractions (30–40% for trichopolyn I and 20–30% for hypelcin A), because the unbound peptides adopt unordered structures (Ref. 11 and Fig. 6) which usually show the amide I′ absorptions near 1645 cm^{-1} [47]. (Here, we assumed that both the concentration and the conformation of the free peptide in the interbilayer aqueous phase are similar to those in the bulk aqueous phase.) Consequently, we can conclude that the helices of these peptides in the membranes distribute randomly or happen to be oriented with angles around the magic angle (54.7°). In contrast, gramicidin, a helical channel-forming peptide, gives a rather high dichroic ratio (4.8) in dimyristoylphosphatidylcholine bilayers [27]. Fringeli and Fringeli reported that alamethicin, an Aib containing icosapeptide analogous to hypelcin A, is perpendicularly oriented to the membrane surface after a hydration-drying procedure (The R value is greater than 5 for a film thinner than the penetration depth) [24]. The orientation of hypelcin A did not change after a gradual drying of the fully hydrated film (data not shown).

Lipid conformation and orientation

The peptide incorporation nonparallel to the membrane normal disordered the lipid acyl chain in the whole temperature region (Fig. 9b). The extent of the disordering by hypelcin A was more significant than that by trichopolyn I. This may be partly ascribed to the larger molecular size of hypelcin A and partly to its

stronger binding to the membrane. These disruptions result from a disordered orientational axis of the lipid, not from an increased gauche conformation because the frequency of the methylene symmetric stretching band did not shift to higher frequencies [19]. Addition of 5 mol% hypelcin A almost never changed the peak position, as in the case of a DMPC-d_{54}/alamethicin (50:1, mol/mol) system [57]. In contrast, incorporation of trichopolyn I fixed the acyl chains in an almost all-trans conformation above the gel to liquid-crystalline phase transition temperature of DPPC. A molecular model shows that if the whole peptide molecule folds into a 3_{10}-helix, the hydrophobic helix just fits the extended acyl chain. The cross sectional area of the helix is approx. 80 Å^2, which is four times larger than that of the saturated hydrocarbon chain. Thus, the two long side chains of the peptide may interact with the two acyl chains of a lipid molecule or the two side chains of a peptide molecule in the opposite leaflet of the bilayer. The disruption of the lipid packing which reduced interlipid interactions in the gel phase will mainly cause the disappearance of the phase transition, as detected by DSC, because the interchain van der Waals interaction, whose change is a major contributor to the phase transition enthalpy change, reduces proportionally to the inverse fifth power of the interchain separation [40]. In the case of the trichopolyn I-DPPC system, the extended acyl chain conformation in the fluid phase also contributes to this phase transition dissipation.

Both peptides appear not to strongly interact with the choline head group of DPPC, in keeping with our NMR study on a hypelcin A-egg yolk phosphatidylcholine system [12]. Peptide–phosphate group interactions were detected by FTIR spectroscopy. Although factors affecting the PO_2^- stretching band contours have not been fully understood, the red shift induced by hypelcin A may indicate a hydrogen bonding between the phosphate group and the hydrogen-donating groups (NH_2 of Gln and OH) in the C-terminal region of the peptide. The blue shift caused by trichopolyn I may reflect a reduced hydration resulting from interactions with the hydrophobic peptide.

Permeability change

Trichopolyn I increased the permeability of phosphatidylcholine bilayers as does hypelcin A (Fig. 3). Our quantitative treatment revealed that the binding of trichopolyn I to egg PC SUVs is expressed as a partition equilibrium with a partition coefficient of $2.0 \cdot 10^3$ M^{-1}, about one-third of that for hypelcin A. The weaker binding of trichopolyn I is consistent with the FTIR data. The linear isotherms suggest that both peptides exist mainly as monomers in the membrane phase, provided that the peptides are monomeric in the aqueous phase. This assumption is compatible with the observation that their conformations in the buffer are concentration independent (up to 50 μM) as revealed by the CD results (see Results and Ref. 11). Alamethicin is well known to form a voltage-gated ion channel [8,58,59]. A channel model based on X-ray diffraction results [49] assumes that several helices aggregate in bundles with their axes parallel to the bilayer normal. Our binding isotherms and FTIR results indicate neither the peptide aggregation nor the parallel peptide orientation. Furthermore, the size of monomeric helical trichopolyn I is too small to span the bilayer. Hydrophobic trichopolyn I cannot form a polar pore, even if the peptide molecules aggregate. Hence, the channel mechanism for the leakage can be excluded. Leakage is not due to vesicle solubilization or fusion for hypelcin A [12] and trichopolyn I (see Results). In conclusion, hypelcin A and trichopolyn I penetrate into the hydrophobic region of the bilayer to enhance the membrane permeability through a common mechanism: membrane-incorporated peptides disrupt lipid packing. However, molecular details, i.e. peptide–phosphate interactions and effects of the peptides on the acyl chain conformations are different. In the case of trichopolyn I, a 'phase separation effect' [60] may contribute to increased membrane permeability in the fluid state. The presence of a transmembrane potential might alter aggregational states, orientations, and conformations of the peptides in membranes [37,61].

Acknowledgment

This work was supported in part by a Grant-in Aid (No. 02453144) for Scientific Research from the Ministry of Education, Science and Culture of Japan.

Appendix

The FTIR-PATR technique, a powerful tool for estimating molecular orientations in an *oriented* sample, has been applied to studies on peptide–lipid interactions [20–22,24,25,27,29]. Although the principle of this method has been reviewed elsewhere [20,22,24,25], we will describe it here briefly, because some confusing discussions have been reported. Fig. A1 illustrates the experimental setup. The molecular orientation can be evaluated from the experimentally obtainable dichroic ratio, R, which is defined as

$$R = \frac{\Delta A_{\parallel}}{\Delta A_{\perp}} = \frac{E_x^2 \cdot k_x + E_z^2 \cdot k_z}{E_y^2 \cdot k_y} \qquad \text{(A-1)}$$

Here, $\Delta A_{\parallel}$ and $\Delta A_{\perp}$ are absorbances of a vibration band, e.g., the methylene symmetric stretching band, for the IR beam with its electric vector parallel (||) and

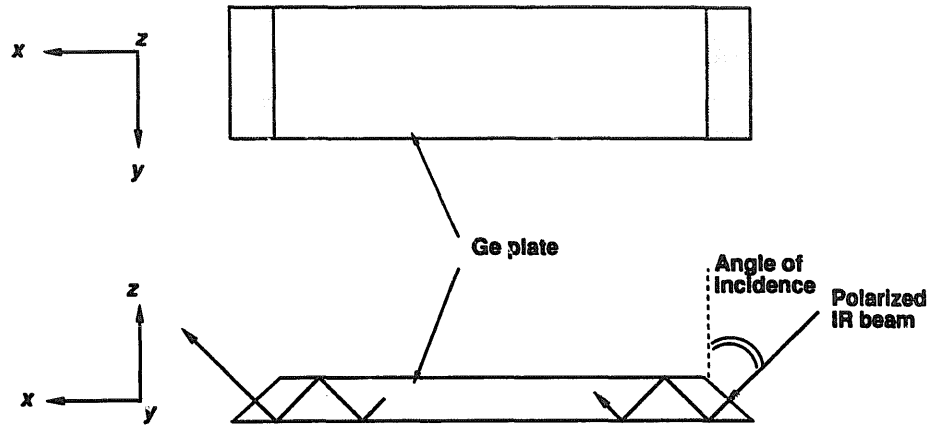

Fig. A1. Experimental setup for the FTIR-PATR experiment. A right-handed coordinate system is defined as illustrated.

perpendicular ($\perp$) to the plane of incidence, respectively. E and k denote the electric field amplitude and the absorption index, respectively, along the x-, y-, or z-axis. It should be noted that in an oriented sample, e.g., lipid films, the intensity of a band, which is proportional to $k_x + k_y + k_z$, must be calculated not from nonpolarized spectra but from polarized spectra using Eqn. A-2 where a uniaxial orientation around the z-axis ($k_x = k_y$) is assumed.

$$k_x + k_y + k_z = a\left\{\frac{1}{E_z^2}\Delta A_{\parallel} + \left(\frac{2}{E_y^2} - \frac{E_x^2}{E_y^2 E_z^2}\right)\Delta A_{\perp}\right\} \qquad \text{(A-2)}$$

Here, a is a constant involving the number of total reflections. This is important, for instance, when one estimates secondary structures of a peptide from its amide I band contour using a curve-fitting procedure.

E values

The thickness of the sample film, d, relative to the penetration depth, d_p [26], is crucial for estimating the E values. In our experimental condition (angle of incidence, 45°; refractive index of lipid film, 1.44; refractive index of germanium, 4.0), d_p is 0.2–0.8 μm in the range 3000–800 cm^{-1}. If $d \gg d_p$, as in our case ($d \approx 6$ μm), the E values can be calculated according to Flournoy-Schaffers' equation [62]. If $d \ll d_p$, they can be estimated as described elsewhere [26]. For a particular orientation, the R values are quite different between both cases. For example, the R values for a randomly oriented vibrating group in a lipid film on a germanium plate (angle of incidence is 45°) are 2.0 and 1.2 in the former and the latter cases, respectively. The latter E values have often been used to evaluate the orientation *without* explicitly stating the film thickness.

k values

Fig. A2 shows a uniaxial orientation model. A molecular axis, e.g., a lipid hydrocarbon chain axis or a peptide helix axis, is assumed to be oriented uniaxially with an angle, α, around the z axis. The transition moment of a particular vibration, e.g., a peptide amide I vibration, is again supposed to distribute uniaxially with an angle, θ, around the molecular axis. In this model, the k values can be correlated to α and θ through Eqns. A-3–A-5.

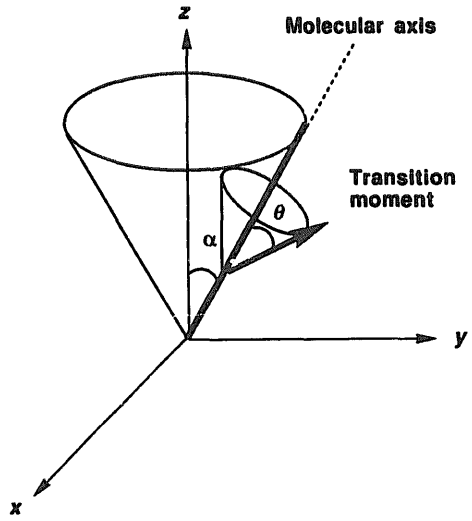

Fig. A2. Uniaxial orientation model. A molecular axis is assumed to be oriented uniaxially with an angle α around the z-axis, the plate normal. The transition moment of a vibration is also presumed to be distributed uniaxially with an angle θ, around the molecular axis.

$$\frac{k_z - k_x}{k_z + 2k_x} = S \cdot S' \qquad \text{(A-3)}$$

$$S = \tfrac{1}{2}(3\cos^2\alpha - 1) \qquad \text{(A-4)}$$

$$S' = \tfrac{1}{2}(3\cos^2\theta - 1) \qquad \text{(A-5)}$$

Here, we used a relation $k_x = k_y$ (uniaxial orientation). S and S' are order parameters of the molecular axis around the z-axis and of the transition moment around the molecular axis, respectively. We can estimate the S value from the observed R value with Eqn. A-6 under

our conditions [27],

$$S \cdot S' = \frac{R - \dfrac{E_x^2 + E_z^2}{E_y^2}}{R - \dfrac{E_x^2 - 2E_z^2}{E_y^2}} = \frac{R - 2.00}{R + 1.45} \qquad \text{(A-6)}$$

The S' value is known for each transition moment, e.g., -0.5 for the methylene symmetric stretching vibration ($\theta = 90°$).

References

1 Fuji, K., Fujita, E., Takaishi, Y., Fujita, T., Arita, I., Komatsu, M. and Hiratsuka, N. (1978) Experientia 34, 237–239.
2 Fujita, T., Takaishi, Y. and Okamura, A. (1981) J. Chem. Soc. Chem. Commun., 585–587.
3 Fujita, T., Takaishi, Y. and Shiromoto, T. (1979) J. Chem. Soc. Chem. Commun., 413–414.
4 Fujita, T., Takaishi, Y., Moritoki, H., Ogawa, T. and Tokimoto, K. (1984) Chem. Pharm. Bull. 32, 1822–1828.
5 Takaishi, Y., Terada, H. and Fujita, T. (1980) Experientia 36, 550–551.
6 Boheim, G., Janko, K., Leibfritz, D., Ooka, T., König, W.A. and Jung, G. (1976) Biochim. Biophys. Acta 433, 182–199.
7 Das, M.K., Raghothama, S. and Balaram, P. (1986) Biochemistry 25, 7110–7117.
8 Eisenberg, M., Hall, J.E. and Mead, C.A. (1973) J. Membr. Biol. 14, 143–176.
9 Irmscher, G. and Jung, G. (1977) Eur. J. Biochem. 80, 165–174.
10 Mathew, M.N., Nagaraj, R. and Balaram, P. (1982) J. Biol. Chem. 257, 2170–2176.
11 Matsuzaki, K., Nakai, S., Handa, T., Takaishi, Y., Fujita, T. and Miyajima, K. (1989) Biochemistry 28, 9392–9398.
12 Matsuzaki, K., Takaishi, Y., Fujita, T. and Miyajima, K. (1991) Colloid Polym. Sci. 269, 604–611.
13 Kanellis, P., Romans, A.Y., Johnson, B.J., Kercret, H. and Chiovetti, R., Jr. (1980) J. Biol. Chem. 255, 11464–11472.
14 Kubesch, P., Boggs, J., Luciano, L., Maass, G. and Tümmler, B. (1987) Biochemistry 26, 2139–2149.
15 Subbarao, N.K., Parente, R.A., Szoka, F.C., Jr., Nadasdi, L. and Pongracz, K. (1987) Biochemistry 26, 2964–2972.
16 Matsuzaki, K., Harada, M., Handa, T., Funakoshi, S., Fujii, N., Yajima, H. and Miyajima, K. (1989) Biochim. Biophys. Acta 981, 130–134.
17 Matsuzaki, K., Harada, M., Funakoshi, S., Fujii, N. and Miyajima, K. (1991) Biochim. Biophys. Acta 1063, 162–170.
18 Amey, R.L. and Chapman, D. (1984) in Biomembrane Structure and Function (Chapman, D., ed.), pp. 199–256, Verlag Chemie, Weinheim.
19 Casal, H.L. and Mantsch, H.H. (1984) Biochim. Biophys. Acta 779, 381–401.
20 Brauner, J.W., Mendelsohn, R. and Prendergast, F.G. (1987) Biochemistry 26, 8151–8158.
21 Cabiaux, V., Brasseur, R., Wattiez, R., Falmagne, P., Ruysschaert, J.-M. and Goormaghtigh, E. (1989) J. Biol. Chem. 264, 4928–4938.
22 Cornell, D.G., Dluhy, R.A., Briggs, M.S., McKnight, C.J. and Gierasch, L.M. (1989) Biochemistry 28, 2789–2797.
23 Fringeli, U.P. (1977) Z. Naturforsch. 32C, 20–45.
24 Fringeli, U.P. and Fringeli, M. (1979) Proc. Natl. Acad. Sci. USA 76, 3852–3856.
25 Fringeli, U.P. and Günnthard, H.H. (1981) in Membrane Spectroscopy (Grell, E., ed.), pp. 270–332, Springer-Verlag, Berlin.
26 Harrick, N.J. (1967) Internal Reflection Spectroscopy, Interscience, New York.
27 Okamura, E., Umemura, J. and Takenaka, T. (1986) Biochim. Biophys. Acta 856, 68–75.
28 Okamura, E., Umemura, J. and Takenaka, T. (1990) Biochim. Biophys. Acta 1025, 94–98.
29 Wald, J.H., Goormaghtigh, E., Meutter, J.D., Ruysschaert, J.-M. and Jonas, A. (1990) J. Biol. Chem. 265, 20044–20050.
30 Ter-Minassian-Saraga, L., Okamura, E., Umemura, J. and Takenaka, T. (1988) Biochim. Biophys. Acta 946, 417–423.
31 Bartlett, G.R. (1959) J. Biol. Chem. 234, 466–468.
32 Allen, T.M. and Cleland, L.G. (1980) Biochim. Biophys. Acta 597, 418–426.
33 Takakuwa, T., Konno, T. and Meguro, H. (1985) Anal. Sci. 1, 215–218.
34 Mao, D. and Wallace, B.A. (1984) Biochemistry 23, 2667–2673.
35 Gordon, D.J. and Holzwarth, G. (1971) Arch. Biochem. Biophys. 142, 481–488.
36 Cascio, M. and Wallace, B.A. (1988) Proteins: Struct., Funct., Genet. 4, 89–98.
37 Rizzo, V., Stankowski, S. and Schwartz, G. (1987) Biochemistry 26, 2751–2759.
38 Vogel, H. (1987) Biochemistry 26, 4562–4572.
39 Yang, J.T., Wu, C.-S.C. and Martinez, H.M. (1986) Methods Enzymol. 130, 208–269.
40 Wilkinson, D.A. and Nagle, J.F. (1981) in Liposomes (Knight, C.G., ed.), pp. 273–298, Elsevier/North-Holland Biomedical Press, Amsterdam.
41 Chapman, D., Cornell, B.A., Eliasz, A.W. and Perry, A. (1977) J. Mol. Biol. 113, 517–538.
42 Gomez-Fernandez, J.C., Goñi, F.M., Bach, D., Restall, C.J. and Chapman, D. (1980) Biochim. Biophys. Acta 598, 502–516.
43 Alonso, A., Restall, C.J., Turner, M., Gomez-Fernandez, J.C., Goñi, F.M. and Chapman, D. (1982) Biochim. Biophys. Acta 689, 283–289.
44 Semin, B.K., Saraste, M. and Wikström, M. (1984) Biochim. Biophys. Acta 769, 15–22.
45 Mendelsohn, R., Anderle, G., Jaworsky, M., Mantsch, H.H. and Dluhy, R.A. (1984) Biochim. Biophys. Acta 775, 215–224.
46 Arrondo, J.L.R., Goñi, F.M. and Macarulla, J.M. (1984) Biochim. Biophys. Acta 794, 165–168.
47 Byler, D.M. and Susi, H. (1986) Biopolymers 25, 469–487.
48 Kennedy, D.F., Crisma, M., Toniolo, C. and Chapman, D. (1991) Biochemistry 30, 6541–6548.
49 Fox, R.O., Jr and Richards, F.M. (1982) Nature 300, 325–330.
50 Bazzi, M.D. and Woody, R.W. (1985) Biophys. J. 48, 957–966.
51 Dwivedi, A.M. and Krimm, S. (1984) Biopolymers 23, 2025–2065.
52 Karle, I.L. and Balaram, P. (1990) Biochemistry 29, 6747–6756.
53 Drake, A.F. and Hider, R.C. (1979) Biochim. Biophys. Acta 555, 371–373.
54 Epand, R.M., Epand, R.F., Orlowski, R.C., Schlueter, R.J., Boni, L.T. and Hui, S.W. (1983) Biochemistry 22, 5074–5084.
55 Epand, R.M., Surewicz, W.K., Highes, D.W., Mantsch, H., Segrest, J.P., Allen, T.M. and Anantharamaiah, G.M. (1989) J. Biol. Chem. 264, 4628–4635.
56 Kaiser, E.T. and Kézdy, F.J. (1984) Science 223, 249–255.
57 Lee, D.C., Durrani, A.A. and Chapman, D. (1984) Biochim. Biophys. Acta 769, 49–56.
58 Boheim, G. (1974) J. Membr. Biol. 19, 277–303.
59 Hall, J.E. and Vodyanoy, I. (1984) Biophys. J. 45, 233–247.
60 Van Hoogevest, P., De Gier, J. and De Kruijff, B. (1984) FEBS Lett. 171, 160–164.
61 Kempf, C., Klausner, R.D., Weinstein, J.N., Renswoude, J.V., Pincus, M. and Blumenthal, R. (1982) J. Biol. Chem. 257, 2469–2476.
62 Flournoy, P.A. and Schaffers, W.J. (1966) Spectrochim. Acta 22, 5–13.